PAPER

Check for updates

Conformational and electronic variability of *N,N',O*-ligand documented on its coordination to main group halides†

Yaraslava Milasheuskaya,[a] Zdeňka Růžičková,[a] Aleš Růžička, [ID][a] Štěpán Podzimek, [ID][b] Roman Jambor [ID][a] and Miroslav Novák [ID] *[c]

The coordination chemistry of non-symmetric ligand **L** (**L** = 2-(C(Me)═N(C$_6$H$_3$-2,6-iPr$_2$))-6-((iPrO)$_2$P═O)C$_5$H$_3$N) is with a focus on its ability to adapt its denticity to accommodate different main-group elements within a potentially tridentate 'pocket' defined by its phosphonate P═O and imine C═N groups together with the pyridine-nitrogen atom. For this purpose, chlorides of groups 13, 14, and 16 were selected, namely InCl$_3$, GeCl$_2$, Ph$_3$SnCl, Ph$_2$SnCl$_2$, SeCl$_4$ and TeCl$_4$. The reaction of **L** with GeCl$_2$ and InCl$_3$ produced [GeCl(**L**)][GeCl$_3$] (**2**) and [InCl$_3$(**L**)] (**5**), respectively. In both compounds, **L** coordinates to the central metal through all its donor atoms with a κ^3-N,N,O-coordination mode. On the contrary, **L** coordinates Ph$_3$SnCl and Ph$_2$SnCl$_2$ through only the phosphonate P═O group, resulting in κ^1-O-coordinated [Ph$_3$SnCl(**L**)] (**3**) and [Ph$_2$SnCl$_2$(**L**)] (**4**). The diverse chelating ability of **L** was found in the reaction with TeCl$_4$ and SeCl$_4$ yielding 2-(C(CH═SeCl$_2$)═N(Dipp))-6-((iPrO)$_2$P═O)C$_5$H$_3$N (**6**) and 2-(C(CH$_2$TeCl$_3$)═N(Dipp))-6-((iPrO)$_2$P═O)C$_5$H$_3$N (**7**) as a result of a C−H bond activation in the Me group of the C(Me)═N fragment. Due to the presence of the M−Cl bond, all compounds **2−7** were subjected to reduction reactions with the aim of synthesising low-valent derivatives. However, only the reduction of **2** with K or KC$_8$ led to the successful isolation of a product, [Ge(**L**)] (**8**). Finally, theoretical studies were carried out to better understand the formation of **6** and **7** as well as the electronic properties of **8**.

Introduction

The design of new neutral ligands has recently become a highly necessary discipline in coordination chemistry. Neutral ligands are mainly used to influence the steric shielding and electronic properties of the metal centre. The interplay of these properties leads to the diverse reactivity of synthesized complexes, which are used as catalysts in organic synthesis. For a successful catalyst, it is essential to stabilise the active metal centre in the complexes. In addition, an open coordination site for interaction of the active metal centre with an organic substrate during the reaction must be made available. From this perspective, non-symmetric neutral ligands containing different donor atoms appear to be suitable candidates for the synthesis of such catalysts. Such systems having donor atoms with very different donating capabilities[1,2] are sometimes termed as hemilabile ligands. This term was coined by Jeffrey and Rauchfuss in 1979 to describe the coordination modes of ligands based on *ortho*-substituted diphenylanisoles.[3] While one donating atom D coordinates strongly, the second atom Z shows a remarkably labile Z/M bond. This labile connection can be cleaved easily, and thus an empty coordination site on the metal can be filled by the incoming organic substrate.

Actually, the consistent architecture of these non-symmetric ligands has allowed the stabilisation of a variety of transition metal (TM) complexes,[4] which have found applications in processes such as carbonylation,[5] alkylation,[6] amination,[7] cross-coupling,[8] olefin methathesis[9] and others.[10] P-block metal complexes with non-symmetric neutral and anionic ligands are uncommon and predominantly employed as catalysts for ring-opening polymerization (Chart 1C and D),[11,12] copolymerization (Chart 1E and F),[13,14] reversible dioxygen binding (Chart 1B),[15] in optoelectronic devices (Chart 1G)[16] and for other specific applications (Chart 1A).[17] The range of utility of non-symmetric ligands heavily relies on the interplay between

[a]Department of General and Inorganic Chemistry, Faculty of Chemical Technology, University of Pardubice, Studentská 573, 53210 Pardubice, Czech Republic
[b]Synpo, Ltd, S.K. Neumanna 1316, 53207 Pardubice, Czech Republic
[c]Institute of Chemistry and Technology of Macromolecular Materials, Faculty of Chemical Technology, University of Pardubice, Studentská 573, 53210 Pardubice, Czech Republic. E-mail: miroslav.novak@upce.cz
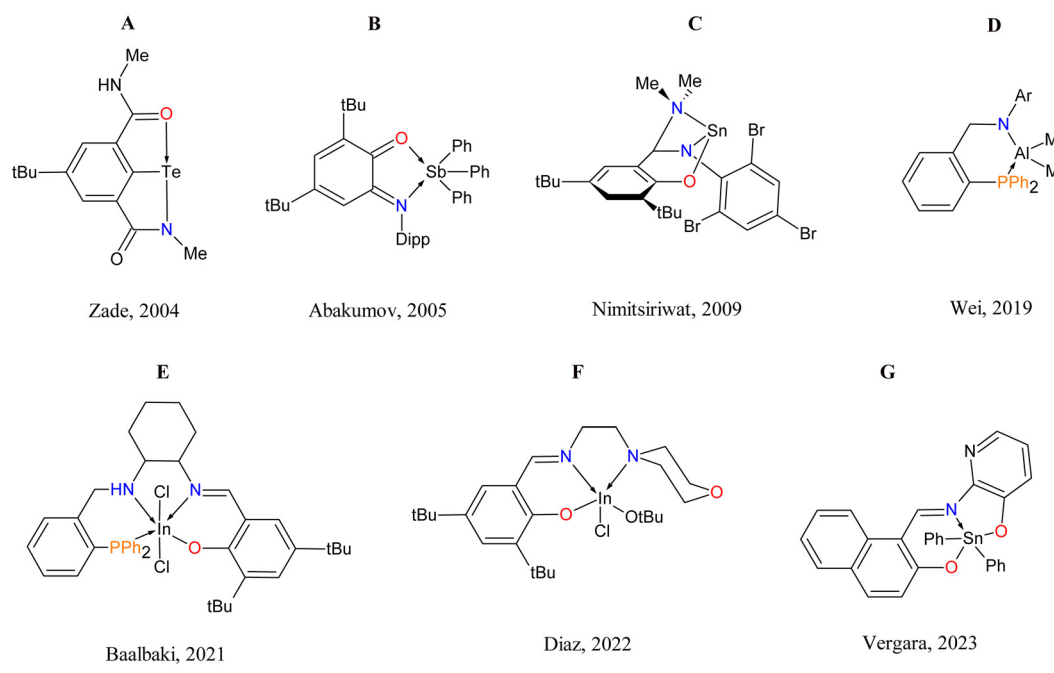
Chart 1 Non-symmetric ligand-stabilized main group metal complexes used as catalysts in organic synthesis.

the properties of the metal and the ligand, and thus employing unsymmetrical ligands has the potential to yield fascinating outcomes owing to their hemilability. For this reason and based on the above, the stabilization of complexes with non-symmetric ligands is a very attractive area of main group metal chemistry.

Very recently, we reported the synthesis of novel non-symmetric neutral N,N′,O-chelating ligands derived from α-imino-(2-(CH═N(C$_6$H$_3$-2,6-iPr$_2$))-6-R-C$_5$H$_3$N) and ketiminopyridine (2-(C(Me)═N(C$_6$H$_3$-2,6-iPr$_2$))-6-R-C$_5$H$_3$N), where R is an additional chelating arm based on ethylphenyl phosphinate (R = Ph(EtO)P═O) and diisopropylphosphite (R = (iPrO)$_2$P═O).[18] These ligands initiated spontaneous autoionization of SnCl$_2$ to give chlorostannyliumylidenes [SnCl (N,N′,O)][SnCl$_3$] (Scheme 1).

Moreover, the presence of an (EtO)P═O or (iPrO)P═O moiety in these non-symmetrical ligands allowed the stabilization of new species[18] due to the elimination of EtCl or iPrCl (Scheme 1B).

While the autoionization reactions of SnCl$_2$ can be initiated by other symmetric or non-symmetric ligands, the elimination

of alkyl chlorides from the parent chlorostannyliumylidene [SnCl (N,N′,O)][SnCl$_3$] is limited to this new type of non-symmetric ligand. These results showed a new reactivity pattern for the aforementioned N,N′,O-chelating ligand **L** (**L** is 2-[C(Me)═N(Dipp)]-6-R-C$_5$H$_3$N, Dipp = C$_6$H$_3$-2,6-iPr$_2$, R = (iPrO)$_2$P═O).

In this study, we report the coordination chemistry of **L** from the point of view of its ability to modify the denticity of a complex and its ability to accommodate different elements inside the potentially tridentate 'pocket' formed when both strong donors—the P═O of phosphonate and the imino group—are orientated on the same side of the complex as the pyridyl nitrogen of the central ring. For this purpose, chlorides of group 13 (InCl$_3$), group 14 (GeCl$_2$, Ph$_3$SnCl, Ph$_2$SnCl$_2$) and group 16 (SeCl$_4$, TeCl$_4$) were chosen to investigate the coordination variability of the ligand **L**.

Results and discussion

Ligand **L** was synthesized *via* the carbon-phosphorus cross-coupling of N-[(6-bromo-2-pyridinyl)ethylidene]-2,6-diiso-propylbenzenamine with diisopropylphosphite according to a previously reported literature method (Scheme 2).[18]

The coordination flexibility of ligand **L** is due to the free rotation of the C(Me)═N(Dipp) and (iPrO)$_2$P═O group around the C–C and C–P bonds, respectively, leading to another three conformers of **L**. We tried to investigate this issue in depth and employed DFT calculations at the M06-2X-D3/def2-TZVP/cpcm (thf) level of theory (Fig. 1). We found that the geometric
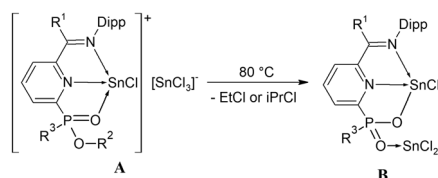
Scheme 1 Representation of the ability of the N,N′,O-chelating ligands to stabilize tin(ɪɪ) cations in a low oxidation state and other species in the form of chlorostannyliumylidenes (**A**) and compound **B**, respectively.
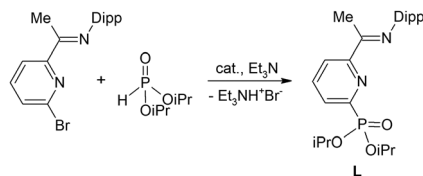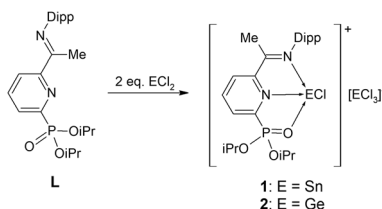
Scheme 2 Synthesis of ligand **L**.[18]
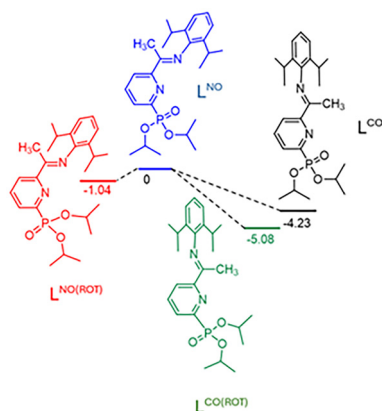
Fig. 1 Low energy conformers of **L** (values in kcal mol^{-1}, calculated at the M06-2X-D3/def2-TZVP/cpcm (thf) level of theory).

structure of the free ligand **L** in its ground state significantly differs from the illustrations shown in Scheme 2. The 180° rotation of the whole phoshonate (iPrO)$_2$P=O group results in an energy gain of 1.04 kcal mol^{-1} (**L**^{NOROT}), while 180° rotation of the C(Me)=N(Dipp) group leads to the species **L**^{CO}, which is 4.23 kcal mol^{-1} lower than the starting point. The combination of both rotations gives the conformer **L**$^{CO(ROT)}$ (ΔG = −5.08 kcal mol^{-1}), where the C=N and P=O groups are oriented to the opposite side of the pyridyl nitrogen of the central ring. However, due to the small energy differences between each conformation, they can transition into each other in solution.

As described previously, the reaction of **L** with 2 molar equiv. of SnCl$_2$ gives the ionic complex [SnCl(**L**)][SnCl$_3$] (**1**) (Scheme 1).[18] Analogously, the reaction of **L** with 2 molar equiv. of GeCl$_2$ provided the ionic complex [GeCl(**L**)][GeCl$_3$] (**2**) (Scheme 3) as the result of the autoionization of GeCl$_2$.

Complex **2** was characterized using multinuclear NMR spectroscopy and single crystal X-ray diffraction analysis. The ^{31}P

{^{1}H} NMR spectrum of **2** revealed a singlet at δ = 14.3 ppm, which is close to the value of the related complex **1** (δ = 16.4 ppm)[18] but shifted downfield compared with the starting ligand **L** (δ = 7.2 ppm) due to the P=O → Ge interaction. The structure of **2** was unambiguously established by the single crystal X-ray diffraction analysis. The molecular structure is depicted in Fig. 2, and the crystallographic data of **2** are summarized in Table S1 (ESI).†

The molecular structure of **2** consists of a well-separated [GeCl(**L**)]$^+$ cation and [GeCl$_3$]$^-$ anion. The Ge1 centre of the [GeCl(**L**)]$^+$ cation is a four-coordinate centre coordinated by the N1, N2, O1 and Cl1 atoms. The O1–Ge1 bond distance (2.261(5) Å), is comparable to those found in related O-coordinated Ge(II) cations (2.13–2.38 Å).[19] Similarly, both the N1–Ge1 (2.145(4) Å) and N2–Ge1 (2.257(5) Å) bond distances fall within the range found in N-coordinated Ge(II) cations stabilized by α-imino and α-ketiminopyridine ligands (2.05–2.55 Å).[20]

Thus, **L** initiates the autoionization of ECl$_2$ (E = Ge, Sn), similar to α-imino and α-ketiminopyridine ligands and behaves as a κ^3-N,N′,O-chelating ligand in the resulting [ECl(**L**)]$^+$ cations. In contrast, the reactions of **L** with 1 or 2 eq. of Ph$_3$SnCl or Ph$_2$SnCl$_2$, other examples of group 14 Lewis acids (LAs), provided neutral complexes [Ph$_3$SnCl(**L**)] (**3**) and [Ph$_2$SnCl$_2$(**L**)] (**4**) (Scheme 4). Compounds **3** and **4** were characterized using multinuclear NMR spectroscopy and single crystal X-ray diffraction analysis.
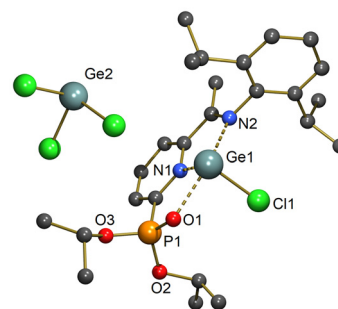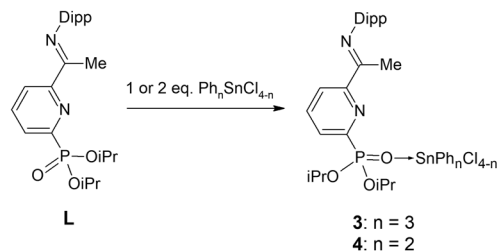

Fig. 2 The molecular structure of **2**. Hydrogen atoms are omitted for clarity. Selected interatomic distances (Å) and angles (°): N1–Ge1 2.145(4), N2–Ge1 2.257(5), O1–Ge1 2.261(5), Ge1–Cl1 2.245(1), P1–O1 1.476(5), N1–Ge1–N2 72.4(2), N1–Ge1–Cl1 93.1(1), N1–Ge1–O1 78.7(2), N2–Ge1–Cl1 88.9(1), N2–Ge1–O1 150.9(2), O1–Ge1–Cl1 89.4(1), P1–O1–Ge1 118.2(2).

Scheme 3 Synthesis of [ECl(**L**)][ECl$_3$] *via* an autoionization reaction.

Scheme 4 Synthesis of neutral complexes [Ph$_3$SnCl(**L**)] (**3**) and [Ph$_2$SnCl$_2$(**L**)] (**4**).

Paper

The $^{31}P\{^1H\}$ NMR spectra of **3** and **4** revealed singlets at δ = 7.6 and 5.3 ppm, respectively, which are close to the signal of the starting ligand **L** but shifted upfield as compared to ionic complexes **1** and **2**. This may suggest a different coordination mode for **L** in these complexes. In addition, the $^{119}Sn\{^1H\}$ NMR spectrum of **3** revealed a singlet at δ = −58.9 ppm, which is comparable to that of the starting complex Ph_3SnCl (δ = −44.7 ppm)[21] and does not fall in the range of −180 to −260 ppm (ref. 22) found for five-coordinated triphenyltin(IV) derivatives. This fact indicates that **3** is kinetically labile on the ^{119}Sn NMR time scale and undergoes dissociation in solution, which is known for related complexes.[23] In contrast, a singlet at δ = −187.7 ppm, found in the $^{119}Sn\{^1H\}$ NMR spectrum of **4**, lies between the signals for the starting Ph_2SnCl_2 complex (δ = −27.2 ppm)[24] and for the five-coordinated $R_3P=O \rightarrow SnPh_2Cl_2$ complexes (R = Et, Bu, n-Oct and Ph; δ = −252 to (−275) ppm).[25] This suggests the presence of a five-coordinated tin atom in **4** with a weak O → Sn coordination in solution.

Single-crystal X-ray diffraction analysis, however, proved the presence of a five-coordinated tin atom in both **3** and **4** in the solid state. The molecular structures are depicted in Fig. 3, and the crystallographic data of **3** and **4** are summarized in Tables S2 and S3 (ESI).†

The molecular structures revealed that the neutral complexes **3** and **4** have Sn1 centre that is five-coordinated and adopts a distorted trigonal bipyramidal arrangement (τ = 0.91 for **3** and 0.80 for **4**). Most importantly, the ligand **L** is coordinated to the tin atom by O → Sn coordination with O1–Sn1 bond distances of 2.447(2) Å (**3**) and 2.2814(15) Å (**4**), which are comparable with those found in an N-(2-pyridinyl) diphenylphosphinic amide → $SnPh_3Cl$ complex (2.4031 Å (ref. 26)). Further, it is evident that neither the pyridine N1 atom nor the imine N2 nitrogen atom is involved in coordination with the tin atom.

From the above results, it is evident that **L** behaves as a κ^1-O-coordinating ligand in the reaction with Ph_3SnCl and Ph_2SnCl_2, which is significantly different from the previous behaviour observed with the ionic compounds **1** and **2**, in which it exhibits κ^3-N,N′,O-chelating behaviour.

This structural variability of **L** also prompted us to employ halides and $InCl_3$, $SeCl_4$, and $TeCl_4$ were tested. While the reaction of **L** with $InCl_3$ provided a neutral complex [$InCl_3(L)$] (**5**), the reaction with $SeCl_4$ and $TeCl_4$ proceeded as C–H activation reactions yielding 2-(C(CH=SeCl$_2$)=N(Dipp))-6-((iPrO)$_2$P=O) C_5H_3N (**6**) and 2-(C(CH$_2$TeCl$_3$)=N(Dipp))-6-((iPrO)$_2$P=O) C_5H_3N (**7**) (Scheme 5). Compounds **5**–**7** were characterized using multinuclear NMR spectroscopy, single crystal X-ray diffraction analysis (**5** and **7**) and MS/MALDI (**6**).

The ^1H NMR spectrum of **5** showed an expected set of signals for **L**. The $^{31}P\{^1H\}$ spectrum of **5** revealed a singlet at δ = 9.3 ppm, which shifted slightly downfield compared with **L** and falls into the range of the ionic κ^3-N,N′,O-coordinated complexes **1** or **2** and neutral κ^1-O-cordinated compounds **3** and **4**. The exact chelation mode was determined by single-crystal X-ray diffraction analysis, which proved that κ^3-N,N′,O-coordination of **L** existed in **5**. The molecular structure is depicted in Fig. 4, and the crystallographic data of **5** are summarized in Table S4 (ESI).†

A different situation was observed for compounds **6** and **7**. The $^{31}P\{^1H\}$ NMR spectra of **6** and **7** revealed a singlet at δ = 4.7 ppm for **6** and δ = 5.0 ppm for **7**, which are shifted upfield compared to κ^3-N,N′,O- and κ^1-O-cordinated compounds. The ^1H NMR spectra of **6** and **7** further revealed the absence of a signal for the methyl groups, which typically resonate at $\delta \approx$
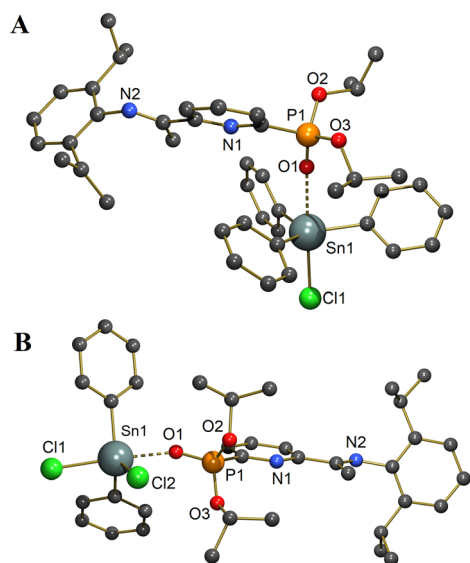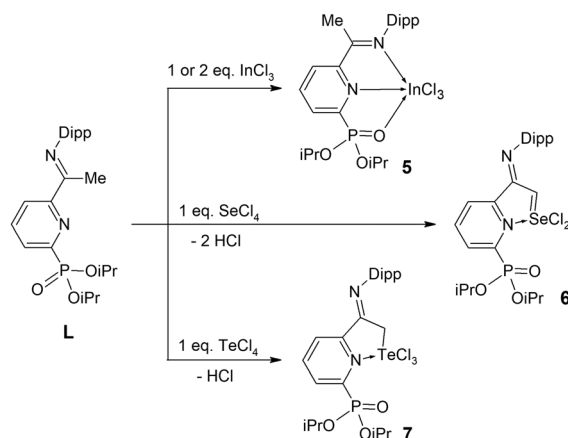

Fig. 3 The molecular structures of **3** (A) and **4** (B). Hydrogen atoms and C_6H_{14} for **3** are omitted for clarity. Selected interatomic distances (Å) and angles (°): (A) for compound **3**: Sn1–Cl1 2.4645(8), Sn1–O1 2.447(2), Sn1–C20 2.136(3), Sn1–C26 2.131(3), Sn1–C32 2.132(3), O1–P1 1.475(2), Cl1–Sn1–O1 175.84(5), C20–Sn1–C26 120.5(1), C20–Sn1–O1 86.0(1), C26–Sn1–Cl1 94.35(9), P1–O1–Sn1 156.71(1); (B) for compound **4**: Sn1–Cl1 2.4511(6), Sn1–Cl2 2.3689(7), Sn1–O1 2.281(1), Sn1–C26 2.134(2), Sn1–C32 2.139(3), O1–P1 1.490(1), Cl1–Sn1–Cl2 90.08(2), C26–Sn1–Cl2 113.25 (5), C26–Sn1–O1 87.18(6), Cl2–Sn1–O1 83.16(4), O1–Sn1–Cl1 173.21(4), P1–O1–Sn1 142.76(9).

Scheme 5 Synthesis of neutral complex [InCl$_3$(L)] (**5**) and C–H activation products 2-(C(CH=SeCl$_2$)=N(Dipp))-6-((iPrO)$_2$P=O)C$_5$H$_3$N (**6**) and 2-(C(CH$_2$TeCl$_3$)=N(Dipp))-6-((iPrO)$_2$P=O)C$_5$H$_3$N (**7**).
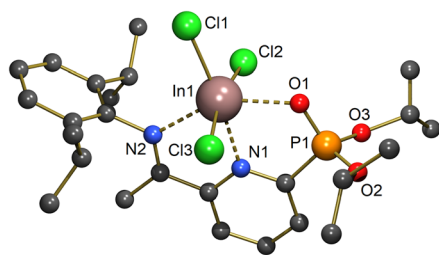
Fig. 4 The molecular structure of **5**. Hydrogen atoms and CH_2Cl_2 are omitted for clarity. Selected interatomic distances (Å) and angles (°): N1–In1 2.279(4), N2–In1 2.362(4), O1–In1 2.255(3), In1–Cl1 2.376(1), In1–Cl2 2.456(1), In1–Cl3 2.457(1), P1–O1 1.480(3), N1–In1–N2 70.1(1), N1–In1–Cl1 173.7(1), N2–In1–O1 147.4(1), Cl2–In1–Cl3 167.96(5), N1–In1–O1 77.4(1), P1–O1–In1 119.1(2).
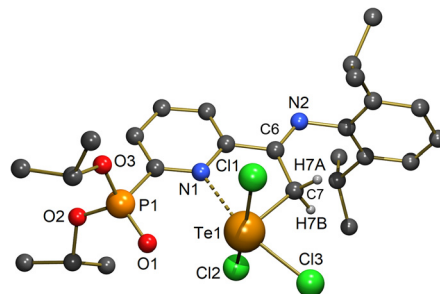

Fig. 5 The molecular structure of **7**. Hydrogen atoms are omitted for clarity. Selected interatomic distances (Å) and angles (°): N1–Te1 2.372(3), O1–Te1 2.862(3), Te1–Cl1 2.491(1), Te1–Cl2 2.504(1), Te1–Cl3 2.454(1), C6–C7 1.512(5), Te1–C7 2.110(3), N1–Te1–Cl3 162.63(9), Cl1–Te1–Cl2 168.36(5), N1–Te1–C7 77.2(1), Cl2–Te1–N1 84.31(9), C6–C7–Te1 77.4(1).

2.3 ppm. In contrast, a new signal at δ = 6.14 ppm, with an integral intensity of 1, was observed in the ^1H NMR spectrum of **6**, while a signal at δ = 4.22 ppm with an integral intensity of 2 was obtained in the ^1H NMR spectrum of **7**. These data indicate the presence of a methine (=CH)C=N proton in **6** and a methylene $(CH_2)C=N$ group in **7**, allowing us to propose the structures of **6** and **7** shown in Scheme 5. Moreover, a signal for the latter is close to a signal found in the structurally related 2-(C(CH$_2$TeX$_3$)=N(Dipp))-6-(CH=N(Dipp))C$_5$H$_3$N (δ = 4.17 ppm when X = Cl, δ = 4.57 ppm when X = Br) prepared by an analogous C–H activation reaction of the DIMPY ligand (DIMPY = 2,6-(C(Me)=N(Dipp)$_2$C$_5$H$_3$N) with TeBr$_4$.[27] The ^1H NMR data were further corroborated by the ^{13}C NMR spectra of **6** and **7**. The ^{13}C NMR spectrum of **6** showed a signal at δ = 62.3 ppm for the (=CH)C=N moiety flanked with ^{77}Se satellites ($^1J(^{77}Se, ^{13}C)$ = 138.5 Hz). A cross peak with the (=CH)C=N signal at δ = 6.14 ppm was also found in the ^1H–^{13}C HSQC experiment. Similarly, the ^{13}C NMR spectrum of **7** revealed a signal at δ = 58.8 ppm for the (–CH$_2$)C=N moiety flanked with ^{125}Te satellites ($^1J(^{125}Te, ^{13}C)$ = 232.6 Hz). The presence of the CH and CH$_2$ moieties was also proved by the ^{13}C APT spectra. Finally, the $^{77}Se\{^1H\}$ NMR spectrum of **6** showed a signal at δ = 1029.7 ppm, while the $^{125}Te\{^1H\}$ NMR spectrum of **7** revealed a signal at δ = 1329.6 ppm, which is comparable with the signal for 2-(C(CH$_2$TeX$_3$)=N(Dipp))-6-(CH=N(Dipp))C$_5$H$_3$N (δ = 1314.7 ppm when X = Cl, δ = 1290 ppm when X = Br).[27] From these data, it is evident that both reactions took place as C–H activation reactions. In the case of SeCl$_4$, the existence of the –N=C=CH– group in **6** indicates that two HCl molecules were eliminated to give the new N=C(CH=SeCl$_2$) moiety, while the (–CH$_2$)C=N group in **7** suggests that the elimination only of one HCl molecule occurred during the formation of N=C(CH$_2$-TeCl$_3$). This was further proved by the MS MALDI TOF spectrum of **6**, where the FTMS$^+$ MALDI MS spectrum showed a signal at m/z 557.12 consistent with the M-Cl fragment of **6** (Fig. S1 in ESI†).

The structure of **7** was unambiguously established *via* single-crystal X-ray diffraction analysis. The molecular structure is depicted in Fig. 5, and the crystallographic data of **7** are summarized in Table S5 (ESI).†

The crystal structure revealed the presence of neutral complex **7**, in which the Te1 centre is five-coordinated and adopts a distorted square pyramidal arrangement (τ = 0.10). Evidence of a new C–Te covalent bond is demonstrated by the C7–Te1 bond distance of 2.110(3) Å (Σ_{cov}C,Te = 2,11 Å),[28] which is slightly shorter than those in {2-[C(CH$_2$TeX$_3$)=N(Dipp)]-6-CH=N(Dipp)-C$_5$H$_3$N} (2.126 Å when X = Cl and 2.133 Å when X = Br).[27] The C7 atom is sp^3 hybridized as demonstrated by the Te–C7–C6 bond angle (114.5(2)°) and by the C7-C6 bond distance (1.512(5) Å) which is close to that of a single bond (Σ_{cov}C, C = 1.50 Å).[28] Most importantly, the ligand **L** is coordinated to the tellurium atom by an N → Te interaction as demonstrated by the N1–Te1 bond distance (2.372(3) Å), which is comparable to those in {2-[C(CH$_2$TeX$_3$)=N(Dipp)]-6-CH=N(Dipp)-C$_5$H$_3$N} (2.321 Å when X = Cl and 2.359 Å when X = Br).[27] The O1–Te1 bond distance of 2.862(3) Å (Σ_{cov}O,Te = 2.02 Å) suggests only a weak interaction, while the remaining imine (N2) nitrogen atom is out of the Te1 coordination sphere. These data thus confirm the presence of a κ^2-C,N'-chelating mode for **L** in **7**.

The presence of the Me substituent on the α-carbon in **L** could be a reason for this different reactivity, allowing for an attack of the C(sp^3)–H bond by TeCl$_4$ and SeCl$_4$. As has been stated, this type of reactivity is known for TeX$_4$ (X = Cl, Br) with DIMPY.[27] For selenium, the reaction of SeCl$_2$ with DIMPY affords an enamine tautomer with an N–H bond, where the N–H proton resonates around 4.5 ppm, and this is the only example of a C(sp^3)–H bond attack.[27b] No signals at this region were observed in the case of the reaction **L** with SeCl$_4$.

In the **L**^{CO} conformation, the ligand **L** coordinates TeCl$_4$ and SeCl$_4$ by its P=O group leading to the formation of **L** → SeCl$_4$ and **L** → TeCl$_4$ with ΔG values of −7.63 and −14.39 kcal mol^{-1}, respectively, (Fig. 6).

Although the O···Se(Te) bond distances in the calculated structures of **L** → SeCl$_4$ and **L** → TeCl$_4$ are 2.387 and 2.220 Å, which are barely below the van der Waals radii of these elements, the Wiberg bond indices (WBI) of 0.129 and 0.230 indicate weaker connections. A suitable orientation of the methyl group towards one of the Se(Te)–Cl fragments then results in a thermodynamically favoured elimination of an HCl

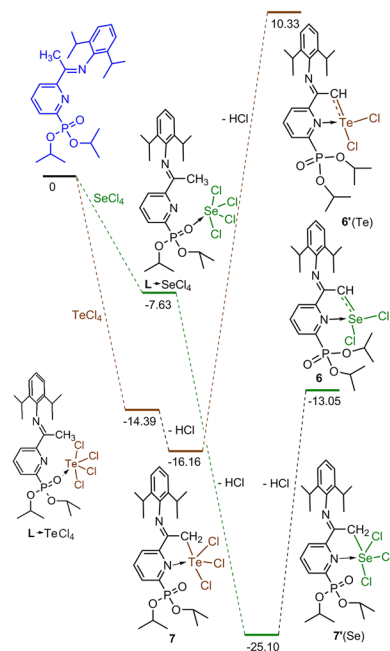**Fig. 6** ΔG profile of the discussed reactions (values in kcal mol^{-1}, calculated at the M06-2X-D3/def2-TZVP/cpcm (thf) level of theory).

molecule and the formation of **7** ($\Delta G = -16.16$ kcal mol^{-1}) and 2-(C(CH$_2$SeCl$_3$)=N(Dipp))-6-((iPrO)$_2$P=O)C$_5$H$_3$N (**7′(Se)**) ($\Delta G = -25.10$ kcal mol^{-1}). While **7** is stable and isolable, **7′(Se)** cannot be isolated because it subsequently loses the second HCl molecule to form **6**. Although the thermodynamic step from **7′(Se)** leading to **6** is endergonic by 12.05 kcal mol^{-1}, the stable structure with a 180° rotated P=O group, the formation of a π-electron conjugated five-membered ring (for orbital representations see Fig. S47 in ESI†) together with the release of a volatile HCl molecule, can force the kinetic pathway of this reaction. The elimination of the second HCl molecule from **7** is also endergonic, but the formation of 2-(C(CH=TeCl$_2$)=N(Dipp))-6-((iPrO)$_2$P=O)C$_5$H$_3$N (**6′(Te)**) is disfavoured as the energy difference (26.49 kcal mol^{-1}) between **7** and **6′(Te)** is much higher than in the case of selenium (12.05 kcal mol^{-1}). For that reason, all attempts to obtain **6′(Te)** led only to a mixture of unidentified products. NBO analysis revealed similar types of HOMO and LUMO for both **7** and **7′ (Se)** (see Fig. S47 in ESI†). While the HOMOs are localized mainly at the Se(Te)–Cl part of the molecules, the LUMOs are found at the hydrogen atoms of the CH$_2$ (and CH$_3$) groups with Cl···H distances of 2.7–2.95 Å. The elimination of HCl molecules from **L** → SeCl$_4$ and **L** → TeCl$_4$ seems to be possible thanks to the orientation, shape and close proximity of the LUMO and HOMO of the molecules, supported by extremely large gaps of ~1.5 eV.

Therefore, the main group metal halides used in this study attacked the various reaction sites of **L** and yielded complexes with different chelating modes ranging from N,N′,O-coordination in either ionic or neutral complexes **1**, **2** and **5**, κ^2-C,N′-coordination as the result of C–H activation in **6** and **7** or κ^1-O-coordination in **3** and **4**.

From this point of view, the reaction employing SeCl$_4$ is quite unique, as the reaction, where two C–H bonds are activated accompanied by the elimination of two HCl molecules is unknown in the literature.

The presence of M–Cl bonds together with different coordination modes of **L** in **1–7** inspired us to test these compounds in reduction reactions with the aim of obtaining low-valent analogues. Unfortunately, the reactions of **1** and **3–7** with Na, K, KC$_8$ or Li[BEt$_3$H] resulted in the elimination of the elemental metal **M** and the free ligand **L**. The only successful reduction occurred for **2** with excess K or KC$_8$, yielding the red-coloured, extremely moisture- and air-sensitive compound [Ge(**L**)] (**8**) (Scheme 6).

Complex **8** was characterized using multinuclear NMR spectroscopy and single crystal X-ray diffraction analysis. The ^{31}P{^{1}H} NMR spectrum of **8** showed a singlet at $\delta = 11.1$ ppm, slightly shifted upfield compared with the starting material **2**. The ^{1}H NMR spectrum of **2** revealed a signal at $\delta = 6.06$ ppm assigned to the pyridine-aromatic hydrogen pyAr–*H* protons. Such a signal was also observed in the ^{1}H NMR spectra of the structurally related species DIMPY → Ge ($\delta = 6.35$ ppm)[29] and DIMPY → Sn ($\delta = 6.23$ ppm).[30] No such signal was observed in the ^{1}H NMR spectrum of **2**, and this upfield-shifted pyAr–*H* signal may suggest a rearrangement and increase of electron density on **L**.

The structure of **8** was unambiguously established by single-crystal X-ray diffraction analysis. The molecular structure is depicted in Fig. 7, and the crystallographic data of **8** are summarized in Table S6 (ESI).†
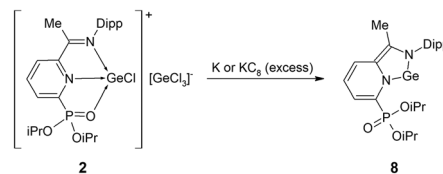
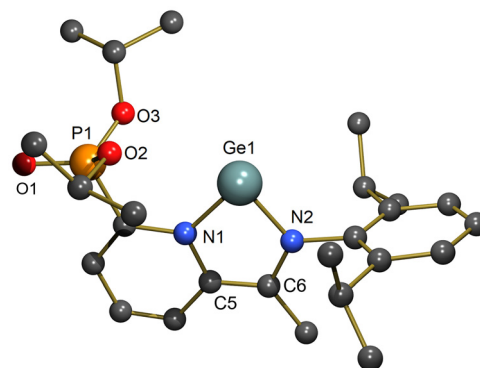**Scheme 6** Synthesis of [Ge(**L**)] (**8**).

Fig. 7 The molecular structure of **8**. Hydrogen atoms are omitted for clarity. Selected interatomic distances (Å) and angles (°): N1–Ge1 1.902 (6), N2–Ge1 1.856(8), O1–Ge1 4.905(6), P1–O1 1.448(7), N1–C5 1.400 (12), C5–C6 1.371(14), C6–N2 1.378(13), N1–C1 1.410(12), N1–Ge1–N2 81.8(3).

The crystal structure revealed the presence of complex **8**, where the ligand **L** coordinates the Ge1 centre by two Ge–N bonds. Thus the [GeCl(**L**)]$^+$ cation in **2** was successfully reduced to [Ge(**L**)] complex **8**. The pyridine nitrogen–germanium bond distance (N1–Ge1 (1.902(6) Å)) is close to that found in [Ge(DIMPY)] (1.8988 Å)[29] and the imine nitrogen–germanium bond distance (N2–Ge1 (1.856(8) Å)) is shorter than those found in the related zero-valent imine → germanium coordination species (range of 1.968–2.907 Å)[29,31] and lies between the single and double covalent bonds ($\Sigma_{cov,SB}$N,Ge = 1.92 Å; $\Sigma_{cov,DB}$N,Ge = 1.71 Å).[28] Moreover, these bond distances are shortened as compared to starting **2** (N1–Ge1 (2.145(6) Å) and N2–Ge1 (2.258(6) Å)). The O1 atom escaped from the coordination sphere of the Ge atom (O1–Ge1 distance 4.905(6) Å) *via* single bond rotation. This may indicate that the [GeCl(**L**)]$^+$ cation in **2** accepts electrons into the structure of the neutral ligand **L** to provide anionic ligand **L**$^{2-}$, while the germanium atom in **8** is still in the +II oxidation state. This fact is not surprising, as related α-iminopyridine ligands are considered as redox non-innocent and can exhibit three redox states—neutral, monoanionic and dianionic.[32]

The structure of **8** was also theoretically investigated using the same approach at the same level of theory as used to investigate **6** and **7**. Geometry optimization provided similar structural parameters to those observed experimentally (see Fig. S51 in ESI).† Fig. S53 and S54† display relevant NBOs of **8** and document the canonical structure with the Ge(II) ion bound by the **L**$^{2-}$ ligand and lone pair of electrons with high *s*-character. Furthermore, the connection is promoted by the donation of lone pairs of electrons from the N1 and N2 atoms (atom names according to those in Fig. 5) and the contribution of a π-bond between the Ge and N1 atom of the pyridyl moiety. In that respect some amount of 3c–4e hypervalent bond character is created between these atoms. WBI (Fig. S52 in ESI†) values for both Ge–N bonds (∼0.63) and bond distances in the ligand core support the compound description.

Conclusions

In conclusion, the coordination chemistry of non-symmetric ligand **L** (2-(C(Me)=N(C$_6$H$_3$-2,6-iPr$_2$))-6-((iPrO)$_2$P=O)C$_5$H$_3$N) was investigated from the point of view of its ability to modify the denticity and accommodation of different elements within the potentially tridentate 'pocket' formed by the P=O of the phosphonate group, C=N of the imine group, and pyridyl nitrogen of the central ring. For this study, various electron-rich chlorides of group 13 (InCl$_3$), group14 (GeCl$_2$, Ph$_3$SnCl, Ph$_2$SnCl$_2$) and group16 (SeCl$_4$, TeCl$_4$) were chosen. Theoretical calculations have shown that, due to the rotation of the C(Me)=N(Dipp) and (iPrO)$_2$P=O groups, **L** is able to exist in four different conformations. This, together with the variability of the donor atoms and Lewis acidity of the studied chlorides, results in multiple coordination modes for **L**. The simplest κ^1-O-coordination was observed for the reactions with Ph$_3$SnCl and Ph$_2$SnCl$_2$, which afforded [Ph$_3$SnCl(**L**)] and

[Ph$_2$SnCl$_2$(**L**)], with the ligand coordinating to the tin atom solely *via* the oxygen of the phosphonate P=O group. Moreover, the different Lewis acidities of Ph$_3$SnCl and Ph$_2$SnCl$_2$ dictate which conformer of **L** coordinates to the given chlorides. While the more acidic Ph$_2$SnCl$_2$ prefers the **L**$^{CO(ROT)}$ conformer, **L**^{CO} was observed in the case of Ph$_3$SnCl. Further, the ligand **L** can act as a κ^3-N,N′,O-chelating ligand, which was demonstrated in the reaction with GeCl$_2$ and InCl$_3$ leading to the auto-ionized [GeCl(**L**)][GeCl$_3$] and neutral [InCl$_3$(**L**)], respectively. The most interesting situation was the experimental observation that electron-rich TeCl$_4$ and SeCl$_4$ react with the ligand to form 2-(C(CH=SeCl$_2$)=N(Dipp))-6-((iPrO)$_2$P=O)C$_5$H$_3$N and 2-(C(CH$_2$TeCl$_3$)=N(Dipp))-6-((iPrO)$_2$P=O)C$_5$H$_3$N as a result of C–H activation of the Me group in the C(Me)=N fragment, which is associated with the elimination of two and one molecules of HCl, respectively. The formation of the selenium species is particularly significant, as similar behaviour is not known in the literature. In this case, ligand **L** behaves as a κ^2-C,N′-chelating species in its **L**^{CO} conformation. The possibility of C–H activation and the number of HCl molecules leaving during the reaction was subsequently studied using theoretical calculations.

Finally, all **L**-coordinated chlorides were subjected to reduction reactions to obtain their corresponding low-valent species. These reactions were only successful for [GeCl(**L**)][GeCl$_3$], where [Ge(**L**)] was obtained. Nevertheless, the structural and theoretical investigations revealed that [Ge(**L**)] is not neutral as initially assumed, as the ligand **L** can accept electron density maintaining the +II oxidation state of the germanium atom. In [Ge(**L**)], the ligand coordinates the germanium atom in a κ^2-N,N-chelating fashion through the **L**$^{NO(ROT)}$ conformation.

Experimental

General considerations

All moisture- and air-sensitive reactions were carried out under an argon atmosphere using standard Schlenk tube techniques. All solvents were dried using Pure Solv–Innovative Technology equipment. Starting compound **L** was prepared according to the literature.[18] GeCl$_2$, Ph$_2$SnCl$_2$, Ph$_3$SnCl, InCl$_3$, SeCl$_4$ and TeCl$_4$ were purchased from Sigma Aldrich and used as received. The ^{1}H, ^{13}C{^{1}H}, ^{31}P{^{1}H}, ^{119}Sn{^{1}H}, ^{77}Se{^{1}H} and ^{125}Te{^{1}H} NMR spectra were recorded on a Bruker 500 NMR spectrometer at 298 K. The ^{1}H and ^{13}C{^{1}H} NMR spectra were referenced internally to the residual protio-solvent. The ^{31}P{^{1}H}, ^{119}Sn{^{1}H}, ^{77}Se{^{1}H} and ^{125}Te{^{1}H} NMR spectra were referenced externally to H$_3$PO$_4$ (85%), Me$_4$Sn, Me$_2$Se and Me$_2$Te. Mass spectra were measured using a LTQ Orbitrap XL MALDI mass spectrometer (Thermo Fisher Scientific, Waltham, MA, USA) with a nitrogen UV laser with a beam size of 80–100 μm. Solid state IR spectra were recorded on a Nicolet 6700 FTIR spectrometer using a single-bounce silicon ATR crystal (resolution 2 cm^{-1}).

DFT calculations

All the calculations were performed with the Gaussian 16 program.[33] The structures were optimized at the DFT level of theory using the M06-2X[34] functional and a standard def2-TZVP[35] basis set with the polarizable continuum model (CPCM) used for implicit tetrahydrofuran solvation.[36] Dispersion corrections were considered, employing the D3 version of Grimme's dispersion method.[37] NBOs and density matrices of natural atomic orbitals (NAO) used for Wiberg bond index analysis were obtained using the NBO 7.0 program.[38]

Synthesis of [{2-(C(Me)═N(Dipp))-6-((iPrO)$_2$P═O)C$_5$H$_3$N} GeCl][GeCl$_3$] (2)

A solution of GeCl$_2$·dioxane (0.22 g, 0.94 mmol) in CH$_2$Cl$_2$ (10 mL) was added to a solution of **L** (0.21 g, 0.47 mmol) in CH$_2$Cl$_2$ (10 mL). The reaction mixture was stirred for 2 h at room temperature. After that, the organic solvent was evaporated under reduced pressure. The residue was washed with a small amount of hexane (10 mL) yielding **2** as an orange powder. Yield: 0.34 g (98%). mp = 144.9 °C. Anal. calcd for C$_{25}$H$_{37}$Cl$_4$O$_3$N$_2$PGe$_2$ (MW 731.62): C, 40.8; H, 5.6. Found: C, 41.0; H, 5.7. ^{1}H NMR (500.13 MHz, CDCl$_3$, 25 °C): δ (ppm) 1.08 (bs, 6H, CH_3(iPr)), 1.19–1.23 (m, 12H, CH_3(iPr) + CH_3(OiPr)), 1.41 (bs, 6H, CH_3(OiPr)), 2.64 (s, 3H, (CH_3)C═N), 2.75 (bs, 2H, CH(iPr)), 4.96 (bs, 2H, CH(OiPr)), 7.26–7.31 (m, 3H, Ar–H), 8.26 (bs, 1H, Ar–H), 8.86–8.90 (m, 2H, Ar–H). ^{13}C{^{1}H} NMR (125.78 MHz, CDCl$_3$, 25 °C): δ (ppm) 19.8 ((CH_3)C═N), 24.0 (CH_3(iPr)), 24.1 (CH_3(OiPr), ^3J(^{31}P, ^{13}C) = 5.2 Hz), 24.3 (CH_3(OiPr), ^3J(^{31}P, ^{13}C) = 2.0 Hz), 25.2 (CH_3(iPr)), 28.7 (CH(iPr)), 29.5 (CH(iPr)), 76.6 (CH(OiPr)), 124.9, 125.2 (^nJ(^{31}P, ^{13}C) = 34.8 Hz), 129.0, 132.0 (^nJ(^{31}P, ^{13}C) = 13.9 Hz), 132.8, 135.0, 141.0 (^nJ(^{31}P, ^{13}C) = 78.3 Hz), 142.2, 146.5, 146.8 (^nJ(^{31}P, ^{13}C) = 8.7 Hz), 149.4 (^nJ(^{31}P, ^{13}C) = 83.5 Hz), 149.6 (Ar–C), 171.1 (C(CH$_3$)═N). ^{31}P{^{1}H} NMR (202.40 MHz, CDCl$_3$, 25 °C): δ (ppm) 14.3. IR: ν(P═O) 1177 cm^{-1}.

Synthesis of {[2-(C(Me)═N(Dipp))-6-((iPrO)$_2$P═O)C$_5$H$_3$N] → SnPh$_3$Cl} (3)

A solution of Ph$_3$SnCl (0.17 g, 0.44 mmol) in C$_6$H$_6$ (10 mL) was added to a solution of **L** (0.20 g, 0.44 mmol) in C$_6$H$_6$ (10 mL). The reaction mixture was stirred for 2 h at room temperature. After that, the organic solvent was evaporated under reduced pressure. The residue was washed with a small amount of hexane (10 mL) yielding **3** as a yellow powder. Yield: 0.34 g (94%). mp = 106.3 °C. Anal. calcd for C$_{43}$H$_{52}$ClO$_3$N$_2$PSn (MW 830.03): C, 62.2; H, 6.3. Found: C, 62.0; H, 6.1. ^{1}H NMR (500.13 MHz, C$_6$D$_6$, 25 °C): δ (ppm) 1.04 (d, 6H, CH_3(iPr), ^3J(^{1}H, ^{1}H) = 6.2 Hz), 1.10–1.12 (m, 12H, CH_3(iPr) + CH_3(OiPr)), 1.14 (d, 6H, CH_3(OiPr), ^3J(^{1}H, ^{1}H) = 6.7 Hz), 2.21 (s, 3H, (CH_3)C═N), 2.80 (sept, 2H, CH(iPr), ^3J(^{1}H, ^{1}H) = 6.2 Hz), 4.63–4.68 (m, 2H, CH(OiPr)), 7.10–7.18 (m, 13H, Ar–H), 7.67 (t, 1H, Ar–H, ^3J(^{1}H, ^{1}H) = 7.1 Hz), 7.78–7.80 (m, 6H, Ar–H), 8.36 (d, 1H, Ar–H, ^3J(^{1}H, ^{1}H) = 7.8 Hz). ^{13}C{^{1}H} NMR (125.78 MHz, C$_6$D$_6$, 25 °C): δ (ppm) 17.8 ((CH_3)C═N), 23.4 (CH_3(iPr)), 24.0

(CH_3(iPr)), 24.3 (CH_3(OiPr), ^3J(^{31}P, ^{13}C) = 5.8 Hz), 24.6 (CH_3(OiPr), ^3J(^{31}P, ^{13}C) = 3.7 Hz), 29.3 (CH(iPr)), 72.4 (CH(OiPr), ^2J(^{31}P, ^{13}C) = 6.8 Hz), 123.8 (^nJ(^{31}P, ^{13}C) = 3.7 Hz), 124.1, 125.0, 128.9, 129.7, 130.6, 136.4, 137.2, 137.4, 140.5, 147.3, 153.3 (^nJ(^{31}P, ^{13}C) = 231.3 Hz), 157.5 (^nJ(^{31}P, ^{13}C) = 22.2 Hz) (Ar–C), 167.4 (C(CH$_3$)═N). ^{31}P{^{1}H} NMR (202.40 MHz, C$_6$D$_6$, 25 °C): δ (ppm) 7.6. ^{119}Sn{^{1}H} NMR (186.49 MHz, C$_6$D$_6$, 25 °C): δ (ppm) −58.9. IR: ν(P═O) 1215 cm^{-1}.

Synthesis of {[2-(C(Me)═N(Dipp))-6-((iPrO)$_2$P═O)C$_5$H$_3$N] → SnPh$_2$Cl$_2$} (4)

The same synthetic protocol was used as for the synthesis of **3**. Ph$_2$SnCl$_2$ (0.11 g, 0.33 mmol) and **L** (0.15 g, 0.33 mmol) provided **4** as a yellow powder. Yield: 0.24 g (93%). mp = 111.2 °C. Anal. calcd for C$_{37}$H$_{47}$Cl$_2$O$_3$N$_2$PSn (MW 788.38): C, 56.4; H, 6.0. Found: C, 56.5; H, 6.1. ^{1}H NMR (500.13 MHz, C$_6$D$_6$, 25 °C): δ (ppm) 0.97 (d, 6H, CH_3(iPr), ^3J(^{1}H, ^{1}H) = 6.2 Hz), 1.07 (d, 6H, CH_3(iPr), ^3J(^{1}H, ^{1}H) = 6.2 Hz), 1.11 (d, 6H, CH_3(OiPr), ^3J(^{1}H, ^{1}H) = 6.8 Hz), 1.14 (d, 6H, CH_3(OiPr), ^3J(^{1}H, ^{1}H) = 6.8 Hz), 2.17 (s, 3H, (CH_3)C═N), 2.79 (sept, 2H, CH(iPr), ^3J(^{1}H, ^{1}H) = 6.2 Hz), 4.73 (bs, 2H, CH(OiPr)), 7.09–7.18 (m, 10H, Ar–H), 7.65 (bs, 1H, Ar–H), 8.08–8.10 (m, 4H, Ar–H), 8.36 (d, 1H, Ar–H, ^3J(^{1}H, ^{1}H) = 8.6 Hz). ^{13}C{^{1}H} NMR (125.78 MHz, C$_6$D$_6$, 25 °C): δ (ppm) 17.7 ((CH_3)C═N), 23.4 (CH_3(iPr)), 24.0 (CH_3(iPr)), 24.1 (CH_3(OiPr), ^3J(^{31}P, ^{13}C) = 5.2 Hz), 24.3 (CH_3(OiPr), ^3J(^{31}P, ^{13}C) = 4.0 Hz), 29.4 (CH(iPr)), 74.1 (CH(OiPr), ^2J(^{31}P, ^{13}C) = 6.0 Hz), 123.8 (^nJ(^{31}P, ^{13}C) = 3.7 Hz), 124.1, 125.0, 128.9, 129.7, 130.6, 136.4, 137.2, 137.4, 140.5, 147.3, 153.3 (^nJ(^{31}P, ^{13}C) = 231.3 Hz), 157.5 (^nJ(^{31}P, ^{13}C) = 22.2 Hz) (Ar–C), 167.4 (C(CH$_3$)═N). ^{31}P{^{1}H} NMR (202.40 MHz, C$_6$D$_6$, 25 °C): δ (ppm) 5.3. ^{119}Sn{^{1}H} NMR (186.49 MHz, C$_6$D$_6$, 25 °C): δ (ppm) −187.7. IR: ν(P═O) 1190 cm^{-1}.

Synthesis of {[2-(C(Me)═N(Dipp))-6-((iPrO)$_2$P═O)C$_5$H$_3$N] → InCl$_3$} (5)

A solution of InCl$_3$ (0.25 g, 1.13 mmol) in THF (10 mL) was added to a solution of **L** (0.50 g, 1.13 mmol) in THF (10 mL). The reaction mixture was stirred for 24 h at room temperature. After that, the organic solvent was evaporated under reduced pressure. The residue was washed with a small amount of hexane (10 mL) yielding **5** as a pale-yellow powder. Yield: 0.71 g (95%). mp = 286 °C (with decomp.). Anal. calcd for C$_{25}$H$_{37}$Cl$_3$O$_3$N$_2$PIn (MW 665.72): C, 45.1; H, 5.6. Found: C, 45.3; H, 5.7. ^{1}H NMR (500.13 MHz, CDCl$_3$, 25 °C): δ (ppm) 1.00 (d, 6H, CH_3(iPr), ^3J(^{1}H, ^{1}H) = 6.4 Hz), 1.19 (d, 6H, CH_3(OiPr), ^3J(^{1}H, ^{1}H) = 5.6 Hz), 1.26 (d, 6H, CH_3(iPr), ^3J(^{1}H, ^{1}H) = 6.4 Hz), 1.39 (d, 6H, CH_3(OiPr), ^3J(^{1}H, ^{1}H) = 5.6 Hz), 2.43 (s, 3H, (CH_3)C═N), 3.25 (sept, 2H, CH(iPr), ^3J(^{1}H, ^{1}H) = 6.4 Hz), 5.24 (m, 2H, CH(OiPr)), 7.19–7.24 (m, 3H, Ar–H), 8.10 (t, 1H, Ar–H, ^3J(^{1}H, ^{1}H) = 6.5 Hz), 8.37–8.42 (m, 2H, Ar–H). ^{13}C{^{1}H} NMR (125.78 MHz, CDCl$_3$, 25 °C): δ (ppm) 19.6 ((CH_3)C═N), 23.9 (CH_3(OiPr), ^3J(^{31}P, ^{13}C) = 7.5 Hz), 24.5 (CH_3(iPr)), 25.4 (CH_3(OiPr), ^3J(^{31}P, ^{13}C) = 16.2 Hz), 28.6 (CH_3(iPr)), 31.3 (CH(iPr)), 68.5 (CH(OiPr)), 125.1, 128.2, 129.1, 130.9 (^nJ(^{31}P, ^{13}C) = 18.6 Hz), 140.1, 140.8, 143.0 (^nJ(^{31}P, ^{13}C) = 10.6 Hz), 144.2 (^nJ(^{31}P, ^{13}C) = 18.6 Hz), 148.1 (^nJ(^{31}P, ^{13}C) = 212.8 Hz)

(Ar–*C*), 166.9 (*C*(CH₃)=N). ³¹P{¹H} NMR (202.40 MHz, CDCl₃, 25 °C): δ (ppm) 9.3. IR: ν(P=O) 1235 cm⁻¹.

Synthesis of {2-[C(CH=SeCl₂)=N(Dipp)]-6-((iPrO)₂P=O)C₅H₃N} (6)

A solution of SeCl₄ (0.14 g, 0.63 mmol) in THF (10 mL) was added to a solution of **L** (0.28 g, 0.63 mmol) in THF (10 mL). The reaction mixture was stirred for 2 h at room temperature. After that, the organic solvent was evaporated under reduced pressure. The residue was washed with a small amount of hexane (10 mL) yielding **6** as an orange powder. Yield: 0.34 g (90%). mp = 180 °C. Anal. calcd for C₂₅H₃₅Cl₂O₃N₂PSe (MW 591.41): C, 50.7; H, 6.0. Found: C, 50.4; H, 5.8. ¹H NMR (500.13 MHz, THF-d8, 25 °C): δ (ppm) 1.04 (d, 3H, C*H₃*(iPr), ³*J*(¹H, ¹H) = 6.7 Hz), 1.25 (d, 6H, C*H₃*(iPr), ³*J*(¹H, ¹H) = 6.7 Hz), 1.29 (d, 3H, C*H₃*(iPr), ³*J*(¹H, ¹H) = 6.8 Hz), 1.32–1.35 (m, 6H, C*H₃*(OiPr), 1.47 (d, 6H, C*H₃*(OiPr), ³*J*(¹H, ¹H) = 6.2 Hz), 2.80 (sept, 1H, C*H*(iPr), ³*J*(¹H, ¹H) = 6.7 Hz), 2.88 (sept, 1H, C*H*(iPr), ³*J*(¹H, ¹H) = 6.7 Hz), 4.84 (m, 1H, C*H*(OiPr)), 4.98 (m, 1H, C*H*(OiPr)), 6.14 (s, 1H, (=C*H*)C=N), 7.18–7.21 (m, 1H, Ar–*H*), 7.25–7.28 (m, 1H, Ar–*H*), 8.31–8.33 (m, 1H, Ar–*H*), 8.38 (bs, 1H, Ar–*H*), 8.43–8.45 (m, 1H, Ar–*H*). ¹³C{¹H} NMR (125.78 MHz, THF-d8, 25 °C): δ (ppm) 22.2 (*C*H₃(iPr)), 22.8 (*C*H₃(iPr)), 24.3 (*C*H₃(OiPr)), ³*J*(³¹P, ¹³C) = 4.7 Hz), 24.4 (*C*H₃(OiPr)), ³*J*(³¹P, ¹³C) = 5.1 Hz), 24.4 (*C*H₃(iPr)), 24.5 (*C*H₃(iPr)), 24.5 (*C*H₃(OiPr)), ³*J*(³¹P, ¹³C) = 4.7 Hz), 24.6 (*C*H₃(OiPr)), ³*J*(³¹P, ¹³C) = 3.7 Hz), 29.4 (*C*H (iPr)), 29.7 (*C*H(iPr)), 62.3 (=*C*H)C=N, (¹*J*(⁷⁷Se, ¹³C) = 138.5 Hz), 73.3 (*C*H(OiPr), ²*J*(³¹P, ¹³C) = 5.6 Hz), 73.4 (*C*H(OiPr), ²*J*(³¹P, ¹³C) = 5.4 Hz), 124.2 (ⁿ*J*(³¹P, ¹³C) = 21.4 Hz), 126.2, 126.2, 126.5, 133.2 (ⁿ*J*(³¹P, ¹³C) = 20.3 Hz), 136.2, 136.8, 141.7 (ⁿ*J*(³¹P, ¹³C) = 11.3 Hz), 144.6, 151.9 (ⁿ*J*(³¹P, ¹³C) = 214.1 Hz), 152.5 (ⁿ*J*(³¹P, ¹³C) = 18.0 Hz) (Ar–*C*), 161.7 (=CH)*C*=N. ³¹P{¹H} NMR (202.40 MHz, THF-d8, 25 °C): δ (ppm) 4.7. ⁷⁷Se{H} NMR (95.34 MHz, THF-d8, 25 °C): δ (ppm) 1029.7. IR: ν(P=O) 1255 cm⁻¹.

Synthesis of {2-[C(CH₂TeCl₃)=N(Dipp)]-6-((iPrO)₂P=O)C₅H₃N} (7)

A solution of TeCl₄ (0.17 g, 0.63 mmol) in THF (10 mL) was added to a solution of **L** (0.28 g, 0.63 mmol) in THF (10 mL). The reaction mixture was stirred for 2 h at room temperature. After that, the organic solvent was evaporated under reduced pressure. The residue was washed with a small amount of hexane (10 mL) yielding **7** as an orange powder. Yield: 0.41 g (87%). mp = 180 °C. Anal. calcd for C₂₅H₃₆Cl₃O₃N₂PTe (MW 677.50): C, 44.3; H, 5.4. Found: C, 44.5; H, 5.6. ¹H NMR (500.13 MHz, THF-d8, 25 °C): δ (ppm) 1.10 (d, 6H, C*H₃*(iPr), ³*J*(¹H, ¹H) = 6.6 Hz), 1.24–1.26 (m, 12H, C*H₃*(iPr) + C*H₃*(OiPr)), 1.44 (d, 6H, C*H₃*(OiPr), ³*J*(¹H, ¹H) = 6.0 Hz), 2.81 (sept, 2H, C*H*(iPr), ³*J*(¹H, ¹H) = 6.6 Hz), 4.22 (s, 2H, (–C*H₂*)C=N), 4.90 (m, 2H, C*H*(OiPr)), 7.14–7.17 (m, 1H, Ar–*H*), 7.23–7.25 (m, 2H, Ar–*H*), 8.32 (t, 1H, Ar–*H*, ³*J*(¹H, ¹H) = 6.6 Hz), 8.57 (bs, 1H, Ar–*H*), 8.84 (d, 1H, Ar–*H*, ³*J*(¹H, ¹H) = 6.6 Hz). ¹³C{¹H} NMR (125.78 MHz, THF-d8, 25 °C): δ (ppm) 23.2 (*C*H₃(iPr)), 24.2 (*C*H₃(OiPr)), ³*J*(³¹P, ¹³C) = 5.4 Hz), 24.3 (*C*H₃(iPr)), 24.5 (*C*H₃(OiPr)), ³*J*(³¹P, ¹³C) = 3.3 Hz), 24.4 (*C*H₃(iPr)), 24.5

(*C*H₃(iPr)), 29.4 (*C*H(iPr)), 58.8 (*C*H₂)C=N, (¹*J*(¹²⁵Te, ¹³C) = 232.6 Hz), 74.7 (*C*H(OiPr), ²*J*(³¹P, ¹³C) = 5.0 Hz), 124.6, 126.5, 128.2 (ⁿ*J*(³¹P, ¹³C) = 2.8 Hz), 133.4 (ⁿ*J*(³¹P, ¹³C) = 17.8 Hz), 135.8, 143.9 (ⁿ*J*(³¹P, ¹³C) = 10.0 Hz), 145.5, 150.4 (ⁿ*J*(³¹P, ¹³C) = 210.2 Hz), 153.1 (ⁿ*J*(³¹P, ¹³C) = 16.4 Hz) (Ar–*C*), 161.0 (–CH₂) *C*=N. ³¹P{¹H} NMR (202.40 MHz, THF-d8, 25 °C): δ (ppm) 5.0. ¹²⁵Te{H} NMR (157.79 MHz, THF-d8, 25 °C): δ (ppm) 1329.7. IR: ν(P=O) 1255 cm⁻¹.

Synthesis of {[2-(C(Me)=N(Dipp))-6-((iPrO)₂P=O)C₅H₃N] → Ge} (8)

Potassium (0.05 g, 1.2 mmol) was added to a solution of compound **2** (0.50 g, 0.68 mmol) in degassed C₆H₆ (20 mL) at room temperature and stirred for 24 h. The solution was filtered from precipitation. After that, the organic solvent was evaporated under reduced pressure, and the dark red solid was dissolved in hexane. The hexane solution was saturated and stored at −20 °C yielding dark red crystals of **8**. Yield: 0.19 g (53%) (mp = 156 °C with decomp.). Anal. calcd for C₂₅H₃₇O₃N₂PGe (MW 517.19): C, 57.6; H, 7.9. Found: C, 57.4; H, 7.6. ¹H NMR (500.13 MHz, C₆D₆, 25 °C): δ (ppm) 1.03 (d, 6H, C*H₃*(iPr), ³*J*(¹H, ¹H) = 6.9 Hz), 1.10 (d, 6H, C*H₃*(iPr), ³*J*(¹H, ¹H) = 6.9 Hz), 1.13 (d, 6H, C*H₃*(OiPr), ³*J*(¹H, ¹H) = 6.1 Hz), 1.26 (d, 6H, C*H₃*(OiPr), ³*J*(¹H, ¹H) = 6.1 Hz), 1.84 (s, 3H, (C*H₃*) C=N), 2.50 (sept, 2H, C*H*(iPr), ³*J*(¹H, ¹H) = 6.9 Hz), 4.73–4.80 (m, 2H, C*H*(OiPr)), 6.02–6.05 (m, 1H, Ar–*H*), 6.91–6.96 (m, 2H, Ar–*H*), 7.12–7.15 (m, 3H, Ar–*H*), 7.19–7.23 (m, 1H, Ar–*H*). ¹³C {¹H} NMR (125.78 MHz, C₆D₆, 25 °C): δ (ppm) 12.4 ((*C*H₃) C=N), 22.9 (*C*H₃(iPr)), 23.6 (*C*H₃(OiPr)), ³*J*(³¹P, ¹³C) = 4.4 Hz), 23.8 (*C*H₃(OiPr)), ³*J*(³¹P, ¹³C) = 3.8 Hz), 26.0 (*C*H₃(iPr)), 27.7 (*C*H (iPr)), 71.2 (*C*H(OiPr)), ²*J*(³¹P, ¹³C) = 5.1 Hz), 116.7 (ⁿ*J*(³¹P, ¹³C) = 14.7 Hz), 119.4 (ⁿ*J*(³¹P, ¹³C) = 17.0 Hz), 124.0, 125.4, 132.4 (ⁿ*J*(³¹P, ¹³C) = 12.0 Hz), 136.4, 138.1, 138.8, 139.7 (Ar–*C*), 145.9 (*C*(CH₃)=N). ³¹P{¹H} NMR (202.40 MHz, C₆D₆, 25 °C): δ (ppm) 11.1. IR: ν(P=O) 1260 cm⁻¹.

Crystallography

Single crystals of **2** were obtained from saturated CH₂Cl₂ solution at −20 °C. Single crystals of **3**·C₆H₁₄ and **4** were obtained from toluene/hexane solutions at −20 °C. Single crystals of **5**·CH₂Cl₂ were obtained from saturated THF solution at −20 °C. Single crystals of **7**·C₆H₁₄ were obtained from saturated toluene/THF solution at −20 °C. Single crystals of **8** were obtained from saturated hexane solution at −20 °C. The X-ray data for the crystals of **2**, **3**·C₆H₁₄, **4**, **5**·CH₂Cl₂, **7**·C₆H₁₄ and **8** were obtained at 150 K using an Oxford Cryostream low-temperature device with a Bruker D8-Venture diffractometer equipped with Mo (Mo/K_α radiation; λ = 0.71073 Å) microfocus X-ray (IμS) source, a Photon CMOS detector and Oxford Cryosystems cooling device was used for data collection. Obtained data were treated by XT-version 2014/5 and SHELXL-2017/1 software implemented in the APEX3 v2016.9-0 (Bruker AXS) system.³⁹ $R_{int} = \sum |F_o{}^2 - F_{o,mean}{}^2|/\sum F_o{}^2$, $S = [\sum(w(F_o{}^2 - F_c{}^2)^2)/(N_{diffrs} - N_{params})]^{\frac{1}{2}}$ for all data, $R(F) = \sum ||F_o| - |F_c||/\sum |F_o|$ for observed data, $wR(F^2) = [\sum(w(F_o{}^2 - F_c{}^2)^2)/(\sum w (F_o{}^2)^2)]^{\frac{1}{2}}$ for all data. Crystallographic data for all structural ana-

lysis have been deposited with the Cambridge Crystallographic Data Centre, CCDC No. 2429433–2429438.†

The frames for all complexes were integrated with the Bruker SAINT software package using a narrow-frame algorithm. Data were corrected for absorption effects using the multi-scan method (SADABS). The structures were solved and refined using the Bruker SHELXTL software package.

Hydrogen atoms were mostly localized on a difference Fourier map. However, to ensure uniformity in the treatment of the crystal, most of the hydrogen atoms were recalculated into idealized positions (riding model) and assigned temperature factors $H_{iso}(H) = 1.2U_{eq}$ (pivot atom) or $1.5U_{eq}$ (methyl). H atoms in the methyl groups, methylene moieties and C–H moieties in aromatic rings were placed with C–H distances of 0.96, 0.97, and 0.93 Å, respectively. Hydrogen atoms in O–H bonds were refined freely.

There are residual electron maxima within the unit cell originating from the disordered solvent (hexane) in the structure of 7, PLATON/SQUEEZE[40] was used to correct the data for the presence of disordered solvent.

Conflicts of interest

There are no conflicts to declare.

Data availability

NMR data and CIF files generated during the study are available at **https://doi.org/10.6084/m9.figshare.29070095**.

Acknowledgements

References

1 (a) R. G. Pearson, *J. Am. Chem. Soc.*, 1963, **85**, 3533; (b) R. G. Parr and R. G. Pearson, *J. Am. Chem. Soc.*, 1983, **105**, 7512.

2 P. Braunstein and F. Naud, *Angew. Chem., Int. Ed.*, 2001, **40**, 680.

3 J. C. Jeffrey and T. B. Rauchfuss, *Inorg. Chem.*, 1979, **18**, 2658.

4 For latest see: (a) K. Schwitalla, L. Gronewold, M. Schmidtmann and R. Beckhaus, *Eur. J. Inorg. Chem.*, 2025, **28**, e202500021; (b) Y. Liao, K. Takahashi and N. Iwasawa, *Organometallics*, 2025, **44**, 189; (c) Y. He, W. Ma, Y. Zhong, Y. Hu, M. Li, F. Zhao, Z. Xia and B. Fan, *Org. Chem. Front.*, 2025, **12**, 569; (d) Z.-Q. Li, T. M. Alturaifi, Y. Cao, M. V. Joannou, P. Liu and K. M. Engle, *Angew. Chem., Int. Ed.*, 2024, **63**, e202411870; (e) B. N. Sánchez-Eguía, H. Hernández-Toledo, S. Lidin, M. Flores-Alamo, E. Nordlander, S. Bertaina, M. Orio and I. Castillo, *ChemCatChem*, 2025, **17**, e202401330; (f) J. C. Wedal, K. B. Virtue, W. H. Bernskoetter, N. Hazari and B. Q. Mercado, *ACS Catal.*, 2024, **14**, 13903; (g) M. Angoy, M. V. Jiménez, E. Vispe and J. J. Pérez-Torrente, *Polym. Chem.*, 2024, **15**, 2028; (h) K. Muratov, E. Zaripov, M. V. Berezovski and F. Gagosz, *J. Am. Chem. Soc.*, 2024, **146**, 3660.

5 (a) K. W. Dong, R. Sang, Z. H. Wei, J. Liu, R. Duhren, A. Spannenberg, H. J. Jiao, H. Neumann, R. Jackstell, R. Franke and M. Beller, *Chem. Sci.*, 2018, **9**, 2510; (b) K. Tanaka, W. R. Ewing and J. Q. Yu, *J. Am. Chem. Soc.*, 2019, **141**, 15494.

6 P. M. P. Garcia, P. Ren, R. Scopelliti and X. L. Hu, *ACS Catal.*, 2015, **5**, 1164.

7 M. V. Jimenez, J. J. Perez-Torrente, M. I. Bartolome, F. J. Lahoz and L. A. Oro, *Chem. Commun.*, 2010, **46**, 5322.

8 (a) S. Handa, J. D. Smith, M. S. Hageman, M. Gonzalez and B. H. Lipshutz, *ACS Catal.*, 2016, **6**, 8179; (b) Z. Q. Weng, S. H. Teo and T. S. A. Hor, *Acc. Chem. Res.*, 2007, **40**, 676.

9 C. S. Higman, D. L. Nascirnento, B. J. Ireland, S. Audorsch, G. A. Bailey, R. McDonald and D. E. Fogg, *J. Am. Chem. Soc.*, 2018, **140**, 1604.

10 (a) H. F. Cheng, A. I. d'Aquino, J. Barroso-Flores and C. A. Mirkin, *J. Am. Chem. Soc.*, 2018, **140**, 14590; (b) E. B. Hulley, M. L. Helm and R. M. Bullock, *Chem. Sci.*, 2014, **5**, 4729; (c) M. S. Rosen, C. L. Stern and C. A. Mirkin, *Chem. Sci.*, 2013, **4**, 4193.

11 N. Nimitsiriwat, V. C. Gibson, E. L. Marshall and M. R. J. Elsegood, *Dalton Trans.*, 2009, 3710.

12 Ch. Wei, B. Han, D. Zheng, Q. Zheng, S. Liu and Z. Li, *Organometallics*, 2019, **38**, 3816.

13 H. A. Baalbaki, K. Nyamayaro, J. Shu, Ch. Goonesinghe, H.-J. Jung and P. Mehrkhodavandi, *Inorg. Chem.*, 2021, **60**, 19304.

14 C. Diaz, J. Fu, S. Soobrattee, L. Cao, K. Nyamayaro, Ch. Goonesinghe, B. O. Patrick and P. Mehrkhodavandi, *Inorg. Chem.*, 2022, **61**, 3763.

15 G. A. Abakumov, A. I. Poddel'sky, E. V. Grunova, V. K. Cherkasov, G. K. Fukin, Y. A. Kurskii and L. G. Abakumova, *Angew. Chem., Int. Ed.*, 2005, **44**, 2767.

16 M. E. Sánchez Vergara, E. Gómez, E. Toledo Dircio, J. R. Álvarez Bada, S. Cuenca Pérez, J. M. Galván Hidalgo, A. González Hernández and S. Hernández Ortega, *Int. J. Mol. Sci.*, 2023, **24**, 5255.

17 S. S. Zade, S. Panda, S. K. Tripathi, H. B. Singh and G. Wolmershäuser, *Eur. J. Org. Chem.*, 2004, 3857.

18 M. Novák, J. Turek, Y. Milasheuskaya, M. Syková, L. Dostál, J. Stalmans, Z. Růžičková, K. Jurkschat and R. Jambor, *Dalton Trans.*, 2023, **52**, 2749.

19 P. A. Rupar, R. Bandyopadhyay, B. F. T. Cooper, M. R. Stinchcombe, P. J. Ragogna, Ch. L. B. Macdonald and K. M. Baines, *Angew. Chem., Int. Ed.*, 2009, **48**, 5155.

20 (a) M. Bouška, L. Dostál, A. Růžička and R. Jambor, *Organometallics*, 2013, **32**, 1995; (b) A. P. Singh,

H. W. Roesky, E. Carl, D. Stalke, J.-P. Demers and A. Lange, *J. Am. Chem. Soc.*, 2012, **134**, 4998; (*c*) E. Magdzinski, P. Gobbo, M. S. Workentin and P. J. Ragogna, *Inorg. Chem.*, 2013, **52**, 11311.

21 A. Lyčka, D. Šnobl, K. Handlíř, J. Holeček and M. Nádvorník, *Collect. Czech. Chem. Commun.*, 1981, **46**, 1383.

22 J. Holeček, M. Nádvorník, K. Handlíř and A. Lyčka, *J. Organomet. Chem.*, 1983, **241**, 177.

23 (*a*) J. Lorberth, S. Wocadlo, W. Massa, E. V. Grigoriev, N. S. Yashina, V. S. Petrosyan and P. Finocchiaro, *J. Organomet. Chem.*, 1996, **510**, 287; (*b*) B. Z. Momeni, S. Shahbazi and H. R. Khavasi, *Polyhedron*, 2010, **29**, 1393; (*c*) K. Gholivand, A. Gholami, S. K. Tizhoush, K. J. Schenk, F. Fadaei and A. Bahrami, *RSC Adv.*, 2014, **4**, 44509.

24 D. Weber, S. H. Hausner, A. Eisengräber-Pabst, S. Yun, J. A. Krause-Bauer and H. Zimmer, *Inorg. Chim. Acta*, 2004, **357**, 125.

25 (*a*) A. Lyčka and J. Holeček, *Inorg. Chim. Acta*, 1986, **122**, 15; (*b*) C. H. Yoder, L. A. Margolis and J. M. Horne, *J. Organomet. Chem.*, 2001, **633**, 33.

26 K. Gholivand, A. Gholami, S. K. Tizhoush, K. J. Schenk, F. Fadaeib and A. Bahrami, *RSC Adv.*, 2014, **4**, 44509.

27 (*a*) G. Reeske and A. H. Cowley, *Chem. Commun.*, 2006, 4856; (*b*) C. D. Martin and P. J. Ragogna, *Inorg. Chem.*, 2012, **51**, 2947.

28 (*a*) P. Pyykkö and M. Atsumi, *Chem. – Eur. J.*, 2009, **15**, 186; (*b*) P. Pyykkö and M. Atsumi, *Chem. – Eur. J.*, 2009, **15**, 12770.

29 T. Chu, L. Belding, A. van der Est, T. Dudding, I. Korobkov and G. I. Nikonov, *Angew. Chem., Int. Ed.*, 2014, **53**, 2711.

30 J. Flock, A. Suljanovic, A. Torvisco, W. Schoefberger, B. Gerke, R. Pöttgen, R. C. Fischer and M. Flock, *Chem. – Eur. J.*, 2013, **19**, 15504.

31 (*a*) B. Su, R. Ganguly, Y. Li and R. Kinjo, *Angew. Chem., Int. Ed.*, 2014, **53**, 13106; (*b*) M. T. Nguyen, D. Gusev, A. Dmitrienko, B. M. Gabidullin, D. Spasyuk, M. Pilkington and G. I. Nikonov, *J. Am. Chem. Soc.*, 2020, **142**, 5852.

32 C. C. Lu, E. Bill, T. Weyhermüller, E. Bothe and K. Wieghardt, *J. Am. Chem. Soc.*, 2008, **130**, 3181.

33 M. J. Frisch, G. W. Trucks, H. B. Schlegel, G. E. Scuseria, M. A. Robb, J. R. Cheeseman, G. Scalmani, V. Barone, G. A. Petersson, H. Nakatsuji, X. Li, M. Caricato, A. V. Marenich, J. Bloino, B. G. Janesko, R. Gomperts, B. Mennucci, H. P. Hratchian, J. V. Ortiz, A. F. Izmaylov, J. L. Sonnenberg, D. Williams-Young, F. Ding, F. Lipparini, F. Egidi, J. Goings, B. Peng, A. Petrone, T. Henderson, D. Ranasinghe, V. G. Zakrzewski, J. Gao, N. Rega, G. Zheng, W. Liang, M. Hada, M. Ehara, K. Toyota, R. Fukuda, J. Hasegawa, M. Ishida, T. Nakajima, Y. Honda, O. Kitao, H. Nakai, T. Vreven, K. Throssell, J. A. Montgomery Jr., J. E. Peralta, F. Ogliaro, M. J. Bearpark, J. J. Heyd, E. N. Brothers, K. N. Kudin, V. N. Staroverov, T. A. Keith, R. Kobayashi, J. Normand, K. Raghavachari, A. P. Rendell, J. C. Burant, S. S. Iyengar, J. Tomasi, M. Cossi, J. M. Millam, M. Klene, C. Adamo, R. Cammi, J. W. Ochterski, R. L. Martin, K. Morokuma, O. Farkas, J. B. Foresman and D. J. Fox, *Gaussian 16, Revision C.01*, Wallingford, CT, 2016.

34 Y. Zhao and D. G. Truhlar, *Theor. Chem. Acc.*, 2008, **120**, 215.

35 F. Weigend, M. Häser, H. Patzelt and R. Ahlrichs, *Chem. Phys. Lett.*, 1998, **294**, 143.

36 V. Barone and M. Cossi, *J. Phys. Chem. A*, 1998, **102**, 1995.

37 S. Grimme, J. Antony, S. Ehrlich and H. Krieg, *J. Chem. Phys.*, 2010, **132**, 154104.

38 K. B. Wiberg, *Tetrahedron*, 1968, **24**, 1083.

39 G. M. Sheldrick, *Acta Crystallogr., Sect. A:Found. Adv.*, 2015, **71**, 3.

40 A. L. Spek, *Acta Crystallogr., Sect. C: Struct. Chem.*, 2015, **71**, 9.